Slow Ligand Binding Kinetics Dominate Ferrous Hexacoordinate Hemoglobin Reactivities and Reveal Differences between Plants and Other Species†

Benoit J. Smagghe,‡,§ Gautam Sarath,|| Emily Ross,|| Jean-louis Hilbert,§ and Mark S. Hargrove*,‡

Department of Biochemistry, Biophysics, and Molecular Biology, Iowa State University, Ames, Iowa 50011, USDA-ARS, University of Nebraska−Lincoln, Lincoln, Nebraska 68583-0937, and Laboratoire de Physiologie de la Différenciation Végétale, Université des Sciences et Technologies de Lille, EA3569-IFR118-ERT1016, Bâtiment SN2, F-59655 Villeneuve d'Ascq Cedex, France

Received September 16, 2005

ABSTRACT: Hexacoordinate hemoglobins are found in many living organisms ranging from prokaryotes to plants and animals. They are named "hexacoordinate" because of reversible coordination of the heme iron by a histidine side chain located in the heme pocket. This endogenous coordination competes with exogenous ligand binding and causes multiphasic relaxation time courses following rapid mixing or flash photolysis experiments. Previous rapid mixing studies have assumed a steady-state relationship between hexacoordination and exogenous ligand binding that does not correlate with observed time courses for binding. Here, we demonstrate that this assumption is not valid for some hexacoordinate hemoglobins, and that multiphasic time courses are due to an appreciable fraction of pentacoordinate heme resulting from relatively small equilibrium constants for hexacoordination (K_H). CO binding reactions initiated by rapid mixing are measured for four plant hexacoordinate hemoglobins, human neuroglobin and cytoglobin, and *Synechocystis* hemoglobin. The plant proteins, while showing a surprising degree of variability, differ from the others in having much lower values of K_H. Neuroglobin and cytoglobin display dramatic biphasic time courses for CO binding that have not been observed using other techniques. Finally, an independent spectroscopic quantification of K_H is presented that complements rapid mixing for the investigation of hexacoordination. These results demonstrate that hexacoordination could play a much larger role in regulating affinity constants for ligand binding in human neuroglobin and cytoglobin than in the plant hexacoordinate hemoglobins.

Hemoglobins (Hbs) with diverse functions are present in all kingdoms of life (*1*−*3*). Oxygen transport in many animals and in the root nodules of nitrogen fixing plants is facilitated by "pentacoordinate" hemoglobins with open heme-iron sites that favor unhindered reversible oxygen binding (*4*). Plants, animals, and some cyanobacteria also contain Hbs that differ from traditional oxygen transport proteins because of a common structural feature: a histidine side chain reversibly binds to the sixth coordination site of the heme iron in both the ferric and ferrous forms of each protein (*5*−*7*). For this reason, these proteins have been termed "hexacoordinate" Hbs (hxHbs). While hxHbs can bind oxygen and other exogenous ligands, kinetic and equilibrium analysis of the reactions is much more complex than the bimolecular reactions observed with pentacoordinate Hbs due to competition from intramolecular coordination of the binding site. While many functions have been proposed for hxHbs from different organisms, and they have the biochemical capabilities to perform many reactions (*4*), no clear role has yet been supported to the exclusion of others (*6*, *8*−*12*).

A basic understanding of ligand binding in hxHbs is important in order to understand their potential physiological functions, and methods have been developed to characterize their kinetic and equilibrium properties (*13*−*15*). Flash photolysis and rapid mixing have been used to examine ligand binding kinetics in many hxHbs, and both techniques have revealed multiphasic time courses for oxygen and carbon monoxide binding that cannot be accounted for using simple reaction models. In an effort to extract useful binding constants, it has been necessary to disregard heterogeneity in reaction time courses (*6*, *11*, *12*, *16*, *17*). For this reason, different binding constants have been reported for some hxHbs that are dependent on how the reactions are initiated or on what time scales they are analyzed (*16*, *17*).

At room temperature, ligand binding to pentacoordinate Hbs is normally monophasic. The bimolecular rate constants observed do not depend on whether rapid mixing or flash photolysis is used to initiate the reaction. Due to this simplicity, kinetic rate constants can be used with confidence to calculate equilibrium constants. However, due to the complexity of reactions in hxHbs, this assumption is tenuous.

† This work was made possible by the National Institutes of Health Award R01-GM065948, support from the Iowa State University Plant Sciences Institute, by a "Contrat Plan-Etat-Région" to the Laboratoire de Physiologie de la Différenciation Végétale, and by a doctoral fellowship of the "Conseil Régional du Nord-Pas de Calais" to Benoit J. Smagghe.

* Correspondence should be addressed to Mark Hargrove, 4114 Molecular Biology Bldg., Ames, IA 50011. E-mail: msh@iastate.edu. Phone: 515-294-2616. Fax: 515-294-0520.

‡ Iowa State University.

|| USDA-ARS, University of Nebraska−Lincoln.

§ Université des Sciences et Technologies de Lille.

10.1021/bi051902l CCC: $33.50
Published on Web 12/16/2005

Kundu et al. (*14*) were unable to reconcile equilibrium constants with kinetic measurements for plant and bacterial Hbs, but Hamdane et al. and Weber et al. have found more success with Ngb (*9*, *18*). Trent et al. (*17*) attempted to formulate a molecular model to account for heterogeneous, slow ligand binding to plant and bacterial hxHbs following rapid mixing. This model proposed a "closed", unreactive form of the protein that accounts for the majority of ligand binding in some cases, but in most others, the binding time courses are much slower than expected from flash photolysis experiments. Therefore, the kinetic events that reveal equilibrium constants for hexacoordination and exogenous ligand binding are still uncertain for many hxHbs.

An understanding of the relationship between kinetics and equilibrium binding is necessary to evaluate potential functions of hxHbs. Presented here is a methodical analysis of hxHbs from plants, animals, and cyanobacteria that compares results from flash photolysis and rapid mixing experiments to a quantitative independent measurement of equilibrium constants for hexacoordination. Our results propose a better model to account for multiphasic ligand binding following rapid mixing and demonstrate that plant hxHbs have distinctly lower equilibrium constants for hexacoordination than their vertebrate and cyanobacterial counterparts.

MATERIALS AND METHODS

Recombinant Protein Production and Purification. Maize hemoglobins (*Zea mays* ssp. *Mays*) Hbm1 and Hbm2 (GeneBank accession number: DQ171946), *Syn*Hb, and Ngb cDNAs were cloned into the expression vector pET28a (Novagen) for recombinant protein production. All proteins were expressed by the host strain BL21 Star DE3 (Invitrogen) except for Ngb, which was expressed by the host strain C41 (Avidis) in a fermentation apparatus described previously (*17*). The expression media consisted of 20 L of Terrific Broth supplemented with 50 μg/mL kanamycin and 1 mL antifoam (Sigma). The strain was cultured at 37 °C with O_2 (0.5 L/min) for 18 h without induction before being harvested by centrifugation (6000 rpm for 4 min). After cell lysis, the proteins were purified by a two-step process: (1) ammonium sulfate fractionation (35−40 and 90%) and (2) immobilized metal affinity chromatography (BD TALON, Clontech). Finally the protein solutions were dialyzed into 10 mM Tris, pH 7.0. The purification efficiency was analyzed with SDS−polyacrylamide gel electrophoresis and spectroscopic analysis of Soret/280 nm ratios (Hewlett-Packard diode array). The other proteins were expressed and purified as described previously (*5*, *19*, *20*).

Kinetic Experiments. Flash photolysis was used to measure the bimolecular CO association rate constant as described previously (*13*). CO and methyl isocyanide (MeICN) binding was measured by rapid mixing using a BioLogic SFM 400 stopped-flow reactor coupled to a MOS 250 spectrophotometer. In a typical experiment, two syringes were used: one containing the protein solution in deoxygenated buffer and the other containing a N_2-equilibrated solution, a CO solution, or a MeICN solution. Both syringes contained 100 μM sodium dithionite. A deoxy-ferrous spectrum was first recorded by mixing 150 μL of the protein solution and 150 μL of the N_2 solution. Time courses were collected at different ligand concentrations by recording the change in absorbance at a fixed wavelength (the Soret maximum, typically 417 nm). At least three kinetic traces were collected and averaged. After the final collection, the final ligand-bound spectrum of the sample was collected.

All rapid mixing experiments were conducted at 20 °C in 100 mM potassium phosphate, pH 7.0. Data analysis and generation of figures employed the software Igor Pro (Wavemetrics, Inc). Equation 2 of Results is discussed extensively as that used for fitting rapid mixing time courses. The form of this equation used in Igor Pro is as follows:

$$\Delta A_{obs} = \Delta A_T \left(\left(\frac{1}{1 + \frac{k_H}{k_{-H}}} \right) e^{-k'_{CO}[CO]^* t} + \left(\frac{\left(\frac{k_H}{k_{-H}}\right)}{1 + \left(\frac{k_H}{k_{-H}}\right)} \right) e^{-k'_{obs,CO}[CO]^* t} \right)$$

This fitting equation results from eq 2 by substituting $F_H = K_H/(1 + K_H)$, $F_P = 1 - F_H$, and $K_H = k_H/k_{-H}$ as described in the first part of Results. Reactions with plant hxHbs exhibited a slower time course of $\sim 1\ s^{-1}$ for ~5% of their respective changes in absorbance. This small fraction of slow binding is addressed in the discussion section. The "closed phase" model equation from Trent et al. used in Figure 2C is calculated using the following equation (as described previously (*17*)):

$$k_{obs,C} = \frac{k_{-H} k_O k'_L [L]}{k_H k_{-O} + k_O[k_{-H} + k_H] + [k_O + k_{-O} + k_{-H}]k'_L[L]}$$

UV−Visible Spectroscopy. A Varian Cary 50 spectrophotometer was used for the imidazole titration of the leghemoglobin mutant H61A. This mutant protein was chosen for the calibration of spectral changes accompanying fractional hexacoordination because it readily binds imidazole in the ferrous form, thus, mimicking hxHbs. The titration was conducted by adding imidazole to the sodium dithionite-reduced protein in 100 mM potassium phosphate, pH 7.0, to achieve concentrations ranging from 0.02 to 1.6 mM. The curve in Figure 7B is fitted to the following equation to extract K_D:

$$F_H = \frac{[\text{imidazole}]}{K_D + [\text{imidazole}]}$$

RESULTS

Kinetic Considerations. The reaction associated with exogenous ligand binding to hxHbs is shown in Scheme 1.

Scheme 1

$$Hb_H \underset{k_H}{\overset{k_{-H}}{\rightleftharpoons}} Hb_P \xrightarrow{k'_L[L]} Hb_L$$

By assuming a steady-state equilibrium between Hb_H and Hb_P, one can derive the following equation for the observed rate of the reaction (*21*):

$$k_{obs,CO} = \frac{k_{-H} k'_{CO}[CO]}{k_H + k_{-H} + k'_{CO}[CO]} \quad (1)$$

This equation predicts an asymptotic approach of k_{obs} to k_{-H} as k'_{CO}[CO] becomes large compared to k_{-H} and k_H, and a linear relationship between k_{obs} and CO when k'_{CO}[CO] $\ll$ k_{-H} and k_H. The equality of this latter relationship is $k_{obs} = k'_{CO}$[CO]/(1 + K_H), where $K_H = k_H/k_{-H}$. Under either circumstance, eq 1 predicts a time course exhibiting a single-exponential phase. These ideas in relation to eq 1 have been discussed previously (*6*, *12*, *13*, *16*, *22*).

However, previous analyses have not considered the situation in which an appreciable fraction of Hb_P is present while k'_{CO}[CO] $\gg$ k_{-H} and k_H. Under these circumstances, two phases are expected in the reaction time course as described by eq 2. In this equation, ΔA_{obs} is the observed

$$\Delta A_{obs} = \Delta A_T[(F_P\, e^{-k'_{CO}[CO]^*t}) + (F_H\, e^{-k'_{obs,CO}[CO]^*t})] \quad (2)$$

time course for binding, $k'_{obs,CO}$ is calculated from eq 1, the fraction of Hb_P and Hb_H are denoted F_P and F_H, $F_H = K_H/(1 + K_H)$, and $F_P + F_H = 1$. ΔA_T is the total change in absorbance expected for the reaction (calculated independently from the ligand-free and ligand-bound absorbance spectra of the protein). Equation 2 predicts biexponential behavior with a fraction of ΔA_T associated with CO binding to F_P and a fraction associated with binding to the hexacoordinate species F_H. The CO concentration dependence of the rate constant describing the reaction with F_P (k'_{CO}) is linearly dependent on [CO], while that of the reaction with F_H would follow eq 1 (as the second term of eq 2).

Three kinetic scenarios are possible for ligand binding to hxHbs in light of this idea. They are discussed here in terms of CO binding but are general for any exogenous ligand.

(1) F_P is Appreciable (K_H < 10) and k'_{CO}[CO] $\gg$ k_{-H} and k_H. Two exponential phases are expected according to eq 2. The fast phase will be linearly dependent on [CO] and the slow phase equal to k_{-H}. The fraction of ΔA_{obs} associated with the slow phase will be equal to F_H, facilitating calculation of K_H from $K_H = F_H/(1 - F_H)$. If k'_{CO}[CO] is greater than the dead time of the mixing apparatus, ΔA_{obs} will be smaller than ΔA_T (due to loss of the bimolecular phase in the mixing dead time), and $\Delta A_{obs}/\Delta A_T = F_H$.

(2) F_P Is Not Appreciable (K_H > 10) and k'_{CO}[CO] $\gg$ k_{-H} and k_H. Under these circumstances ΔA_{obs} will be equal to ΔA_T for all [CO]. A single-exponential phase will be observed that is equal to k_{-H}.

(3) k'_{CO}[CO] Is Not $\gg$ k_{-H} and k_H. Equation 1 (or the second term of eq 2) describes binding under these conditions, as the bimolecular reaction is not fast enough to sample the relative populations of Hb_P and Hb_H. Time courses will be single-exponential and dependent on [CO] as described for eq 1.

With eq 2 and these scenarios in mind, a set of binding time courses that vary in [CO] can, in some cases, define k_{-H}, k_H, and K_H by examining not only the observed rate constants but also the change (or loss) in amplitude associated with the reaction. At very least they can elucidate the relationship between rate constants described in each kinetic scenario.

CO Binding to SynHb. Ligand binding time courses following flash photolysis of CO-bound *Syn*Hb are clearly biphasic, with both phases dependent on CO concentration (Figure 1A) (*16*). When initiated by flash photolysis, the reaction is over in less than 0.1 s. We have shown previously that integration of Scheme 1 (with $Hb_{total} = Hb_P$ at $t = 0$) predicts two phases of rebinding following flash photolysis (*13*). Using this method and analyzing the two phases shown, Hvitved et al. (*16*) assigned rate constants for k'_{CO}, k_H, and k_{-H} as 90 μM^{-1} s^{-1}, 4200 and 930 s^{-1}.

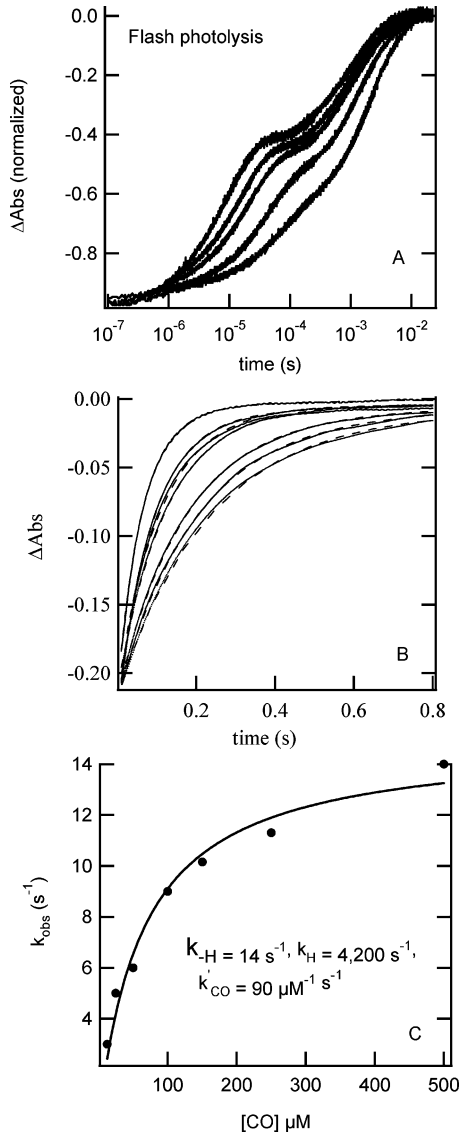

FIGURE 1: CO binding to *Syn*Hb. (A) Time courses for CO rebinding to *Syn*Hb following flash photolysis at different CO concentrations (100−1000 μM, right to left). The time courses are clearly biphasic, both phases being dependent on the CO concentration. (B) Time courses for CO binding to *Syn*Hb following rapid mixing at different CO concentrations (12.5−500 μM, right to left). Exponential fitted curves are shown as gray dashed lines. (C) CO dependence of the rate constant for binding to *Syn*Hb. The data are fitted to eq 1 to extract k_H and k_{-H}.

An alternative method of initiating the binding reaction is rapid mixing in a stopped-flow apparatus. Time courses for CO binding to *Syn*Hb following rapid mixing are shown in Figure 1B. In contrast to Figure 1A, these reactions require over a second to reach completion at lower [CO]. In light of eq 2, the first point to notice about this collection of time courses is that each one is largely single exponential and exhibits the complete expected amplitude for the reaction (this is consistent with Kinetic Scenarios 2 and 3). The fact that the observed rate constants increase with CO is consistent only with Scenario 3, in which k'_{CO}[CO] is not so

Table 1: Ligand and Hexacoordination Rate Constants

	k'_{CO} ($\mu M^{-1} s^{-1}$)	k_H (s^{-1})	k_{-H} (s^{-1})	K_H	fraction hex	A_{555}/A_{540}
riceHb1	6.8	75	40	1.9	0.65	1.91
riceHb2	1.8	6.7	15	0.45	0.3	1.33
MHb1	1.4	22	25	0.9	0.48	1.8
MHb2	44	43	19	2.3	0.70	2.30
*Syn*Hb	90	4200	14	300	~1	2.35
Ngb	40	≥2000*	2.3 (70%) 0.2 (30%)	~1000	~1	2.22
Cgb	5.6	430	0.5 (70%) 0.09 (30%)	860	~1	2.33

large as to remove the concentration dependence from eq 1. The rate constants extracted from these time courses are plotted versus [CO] in Figure 1C. The values approach an asymptote of ~14 s^{-1}. If the values of k_H and k'_{CO} are fixed from analysis of flash photolysis data, the solid curve in Figure 1C results from a fit to eq 1 with k_{-H} as the fitted variable. These values are reported in the inset to Figure 1C and in Table 1.

CO Binding in Plant hxHbs: RiceHb1. Heterogeneous CO binding in hxHbs first focused on a plant hxHb from rice (riceHb1) (*13*, *14*). Like *Syn*Hb, multiphasic ligand binding time courses following flash photolysis are observed, and hexacoordination rate constants have been calculated from that experiment (*13*). Extensive analysis of CO binding to riceHb1 following rapid mixing was also reported in an effort to explain multiphasic time courses (*17*). The model resulting from the previous rapid mixing study implicated a "closed", unreactive form of the protein to explain aspects of the binding time course that were not expected from the flash photolysis results. However, the "closed-form" model could account for only ~60% of the binding time course for riceHb1 at low [CO], and even less for higher [CO] and other hxHbs.

Here, we demonstrate that eq 2 provides a better interpretation for analysis of binding time courses initiated by rapid mixing. Figure 2A shows time courses for CO binding to riceHb1 (from 12.5 to 500 μM) with the *y* axis normalized to the expected change in absorbance ($\Delta A_T = 1$). The early parts of these time courses are shown in expanded detail in Figure 2B. It is evident that there is a fast phase for binding that results in amplitude loss in the dead time of the reaction at higher concentrations of CO. This behavior is consistent with the Scenario 1 predicted by eq 2 with k'_{CO}[CO] approaching the dead time of the reaction.

At the highest [CO], $k_{obs} = 40$ s^{-1}, which is ~k_{-H}. With this value and k'_{CO} fixed at 6.8 μM^{-1} s^{-1} (from flash photolysis (*13*, *23*)), each time course can be fit to eq 2 with k_H as the fitted parameter, yielding a value of 75 s^{-1}. As noted in Materials and Methods, the formulation of eq 2 is affected by k_H in the second exponential term (as part of eq 1), and in defining the relative amplitudes associated with binding to F_P and F_H. Thus, if $\Delta A_{obs} \neq \Delta A_T$ (as in this case), the definition of k_H is very robust, as it results from two independently measurable aspects of each time course.

A comparison of the ability of eq 2 and the previous "closed phase" model (*17*) to account for these time courses is provided in Figure 2C (this fitting equation is provided in Materials and Methods). The fitted curves are calculated from the rate constants provided in Trent et al. (*17*). The poor fit at longer time scales and higher [CO] was an admitted

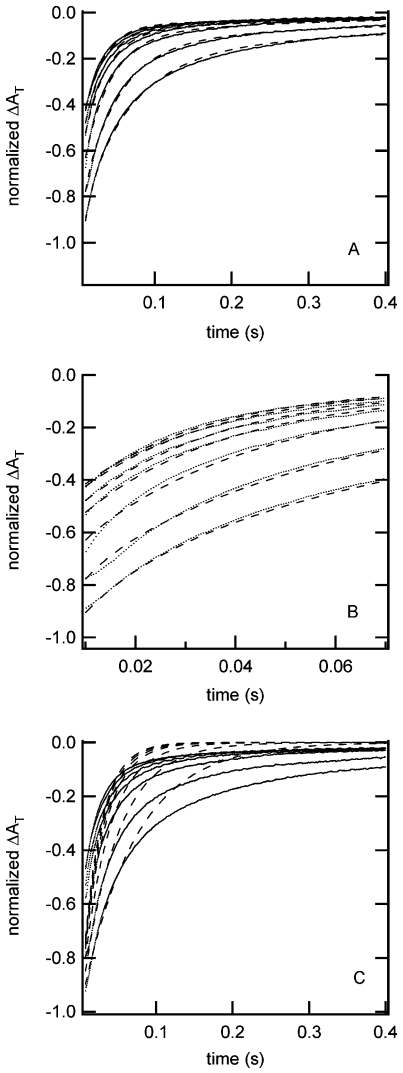

FIGURE 2: CO binding to RiceHb1. (A) Time courses for CO binding to RiceHb1 following rapid mixing at different CO concentrations (12.5−500 μM, right to left). (B) The data in panel A are expanded to facilitate observation of the starting time points of the reaction. In this and in panel A, the fitted curves are gray dashed lines and result from the use of eq 2 to describe each time course. (C) The data are fitted to the model described earlier (*17*). The fits in panels A and B are clearly superior to those in panel C.

weakness of this model and is drastically improved by fitting to eq 2 (Figure 2A,B). Therefore, the ability of eq 2 to account for F_P provides a much better fit to, and a simpler mechanistic explanation for, multiphasic time courses for ligand binding than the previous model. An additional benefit is the ability of eq 2 to exploit lost amplitude in the reaction to provide an independent estimate of K_H.

CO Binding to RiceHb2. Rice (*Oryza sativa*) contains at least two Hbs, which share 92% identity. Here, we use the methods described above to measure CO binding to riceHb2 to address the question of whether its properties are like those of riceHb1. Unlike riceHb1, riceHb2 exhibits single-exponential CO rebinding following flash photolysis (Figure 3A). A single-exponential decay is used to fit the CO binding time courses, and a rate constant (k_{obs}) is extracted for each [CO]. The plot of k_{obs} versus [CO] is shown in Figure 3B, and the slope of the linear fit gives us k'_{CO} equal to 1.8 μM^{-1} s^{-1}. These results suggest $k_H \ll k'_{CO}$[CO], such that very little competition for CO rebinding is provided by the internal His side chain (*13*).

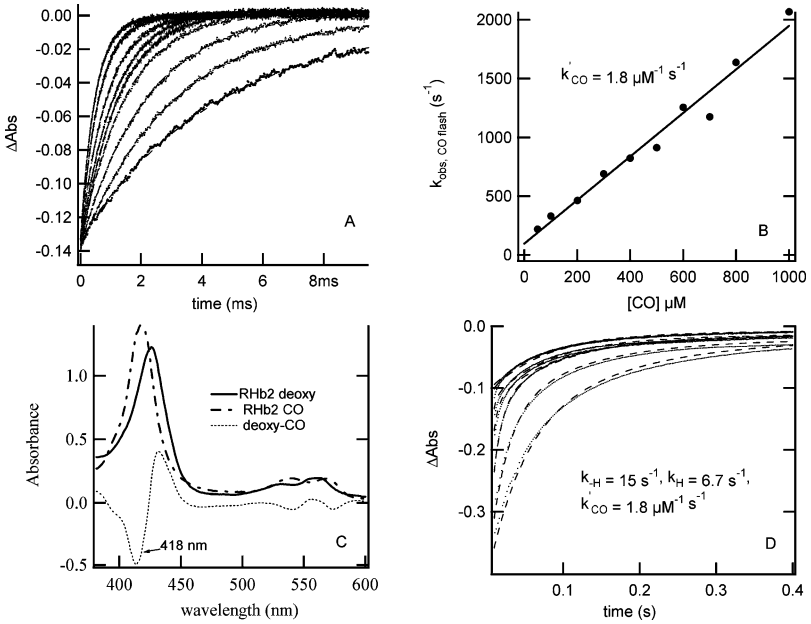

FIGURE 3: CO binding to RiceHb2. (A) Time courses for CO rebinding following flash photolysis are singe-exponential and dependent on [CO] (100−1000 μM, right to left). (B) Fitted rate constants from panel A are plotted versus [CO] to provide k'_{CO}. (C) The difference spectrum (dotted line) between the deoxy (solid line) and CO spectra (dashed line) as observed in the stopped-flow reactor is used to calculate ΔA_T for eq 2. (D) Time courses for CO binding to riceHb2 following rapid mixing at different CO concentrations (12.5−500 μM, right to left). The data are fitted (gray dashed lines) to eq 2 with a k'_{CO} fixed at 1.8 μM^{-1} s^{-1}, and k_{-H} taken from the time course at 500 μM CO.

However, CO binding following rapid mixing is more complex (Figure 3C,D). Quantification of the time courses requires at least two exponential terms, and only a fraction (0.3) of ΔA_T (Figure 3D) is observed at higher [CO]. As was the case for riceHb1, this behavior cannot be simply explained by the reaction model leading to eq 1 but is readily interpreted using eq 2 and Scenario 1. Therefore, from the fraction of slow phase remaining (0.3) and the rate constant extracted from this time course (15 s^{-1}), we obtain K_H and k_{-H}, respectively. The rest of the reaction is due to F_P reacting rapidly (at least compared to k_H) with CO. The lost amplitude at higher [CO] results from k'_{CO}[CO] approaching the reaction dead time, while at lower [CO], the full amplitude is observed. With k'_{CO} measured from flash photolysis, and with K_H and k_{-H} measured at high [CO] by rapid mixing, k_H can be extracted from fits of eq 2 to each time course in Figure 3D. These are the values for each rate constant that give rise to the fitted curves shown in this figure and in Table 1.

CO Binding to Maize Hbs (Hbm1 and Hbm2). Like rice, maize (*Zea mays* ssp. *mays*) contains two hxHbs that share 60% identity with each other and between 80% (Hbm1) and 60% (Hbm2) identity with the hxHbs from rice. In the case of Hbm1, the time courses for CO binding following flash photolysis fit to single-exponential decays similar to those of riceHb2. The plot of k_{obs} versus the [CO] is shown in Figure 4A. The slope of the linear fit is the CO bimolecular rate constant (k'_{CO}) and is equal to 1.4 μM^{-1} s^{-1}. When the reaction is monitored by rapid mixing, the results are again comparable to riceHb1 and riceHb2, showing loss of amplitude as [CO] increases (Figure 4C). As [CO] is increased (up to 500 μM), the observed amplitudes decrease (~50%), indicating that the hexacoordinate fraction is equal to 0.5, with a $K_H = 1$. The values for k_H and k_{-H} resulting from this analysis fall between those of the two rice proteins (Figure 4C, Table 1).

Results from analysis of Hbm2 are shown in Figure 5. Surprisingly, Hbm2 exhibits a significantly larger bimolecular rate constant for CO binding (Figure 5A). The value of 44 μM^{-1} s^{-1} is closer to that of *Syn*Hb than the other plant hxHbs. This rate constant is one of the fastest among plant hxHbs and is comparable to human Ngb (*6*). With such a large value of k'_{CO}, one would expect a significant loss in amplitude in the mixing experiment if F_P were appreciable. However, panels B and C of Figure 5 show that this is not the case. ΔA_T for the reaction at this concentration of protein is shown in Figure 5B to be 0.22. The observed amplitudes range from 0.2 to 0.15, coalescing at the lower value at higher [CO]. k_{obs} at the highest [CO] is 43 s^{-1}, which is assigned to k_{-H}. This value, in combination with $k'_{CO} = 44$ μM^{-1} s^{-1}, was fixed in eq 2 and used to fit the time courses in Figure 5C to extract a value of 19 s^{-1} for k_H. The value of K_H resulting from these rate constants is 2.3, indicating F_H equal to 0.7. Under these circumstances, F_H multiplied by ΔA_T should (and does) equal ΔA_{obs}, which is 0.15 at all [CO].

Ligand Binding in Human hxHbs. We have demonstrated in the previous sections that eq 2 provides a superior explanation for complex time courses for ligand binding to plant and cyanobacterial hxHbs following rapid mixing. From reaction Scheme 1, only two exponential phases are expected for ligand rebinding following flash photolysis. However, multiphasic, heterogeneous time course have been reported for the human hxHb Ngb that have led to confusion in the analysis of ligand binding in this protein. For example, Trent et al. (*6*) and Dewilde et al. (*12*) reported comparable values of k_H and k'_{CO} for Ngb, but the value of k_{-H} reported by Trent et al. was ~1000 times faster than that reported by Dewilde et al. Both groups used flash photolysis for analysis, and both saw heterogeneity on fast time scales. Others have also reported multiphasic ligand rebinding following flash photolysis (*9*, *10*, *12*, *24*).

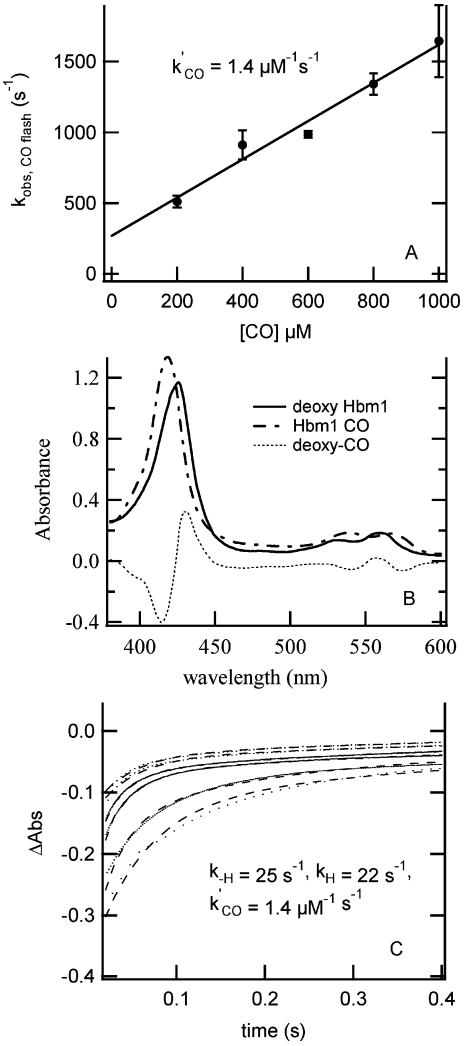

FIGURE 4: CO binding to maize Hbm1. (A) Rate constants for CO binding are measured from flash photolysis and plotted versus the CO concentration to provide k'_{CO}. (B) The difference spectrum (dotted line) between the deoxy (solid line) and CO spectra (dashed line) as observed in the stopped-flow reactor is used to calculate ΔA_T for eq 2. (C) Time courses of CO binding to Hbm1 following rapid mixing at different CO concentrations (12.5−500 μM, right to left). The data are fitted to eq 2 with a k'_{CO} fixed at 1.4 μM^{-1} s^{-1} and k_{-H} taken from the time course at 500 μM CO.

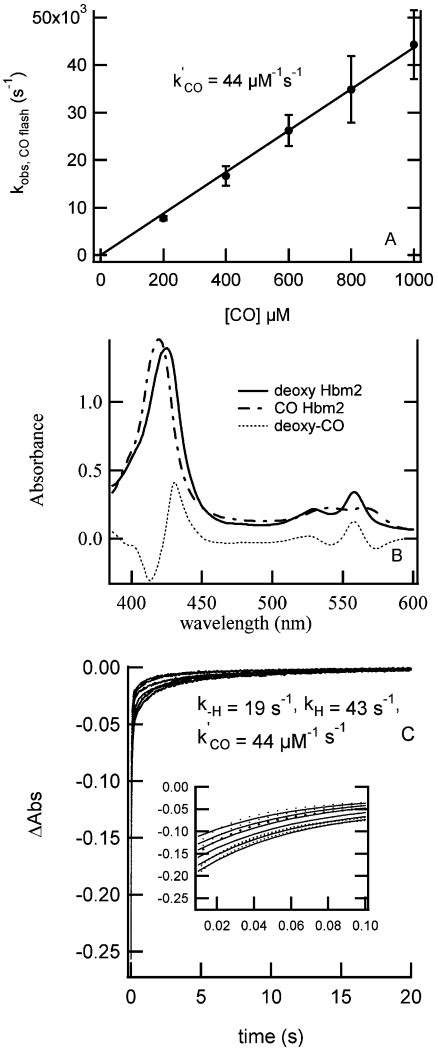

FIGURE 5: CO binding to maize Hbm2. (A) As for the Hbm1 and riceHb2, flash photolysis is single-exponential and provides k'_{CO}. (B) The difference spectrum (dotted line) between the deoxy (solid line) and CO spectra (dashed line) as observed in the stopped-flow reactor is used to calculate ΔA_T for eq 2. (C) Time courses for CO binding to Hbm2 following rapid mixing at different CO concentrations (12.5−500 μM, right to left). The inset shows these time courses at an expanded time scale to demonstrate ΔA_{obs}. The data are fitted to eq 2 with a k'_{CO} fixed at 1.4 μM^{-1} s^{-1} and k_{-H} taken from the time course at 500 μM CO.

Here, we are interested in using rapid mixing and eq 2 to analyze ligand binding to the two human hxHbs, Ngb and Cgb, to reconcile these differences. Analysis of the faster phases of binding (as in Trent et al. (*6*)) yields a larger value of k_{-H} and, thus, a smaller value for K_H and F_H. Alternatively Dewilde et al. (*12*) and Nienhaus et al. (*11*) focused on slower binding and reported slower values of k_{-H} and larger values of K_H. The experiments reported here are ideally suited to distinguish between these two possibilities. If K_H is large (and k_H slow), rapid mixing time courses should be independent of [CO] and fit to a single-exponential term, thus, appearing more similar to those for Hbm2 in Figure 5 (conforming to Scenario 2). If K_H is smaller (and k_H faster), the collection of data should more closely resemble that of the other plant hxHbs (conforming to Scenario 1).

Panels A and B of Figure 6, show CO binding following rapid mixing to Ngb and Cgb, respectively, with the ordinate axes normalized to ΔA_T for the reaction. For both proteins, the expected ΔA_T is observed at each [CO]. However, the time courses are markedly biphasic. Ngb time course fit to 2.3 s^{-1} (70%) and 0.2 s^{-1} (30%), and Cgb to 0.5 s^{-1} (70%) and 0.085 s^{-1} (30%). To demonstrate the necessity of the biphasic fits, single-exponential time courses simulating 100% fast (dashed) and 100% slow phase (dotted) binding for each protein, respectively, are included in Figure 6.

As time courses are the same at each [CO], and $\Delta A_{obs} = \Delta A_T$, these data support Scenario 2 for both proteins. The rate constants observed at each [CO] for Ngb and Cgb are thus best interpreted as k_{-H}. The value reported here for Ngb is much closer to that reported by Dewilde et al. (*12*) (4.5 s^{-1}) than that reported by Trent et al. (*6*). However, neither previous study revealed the fraction of binding occurring at <1 s^{-1} that accounts for 30% of the reaction time course, and the second phase of binding is not expected with Scenario 2. One possible explanation for these two fractions is the potential of both Ngb and Cgb to form internal disulfide bonds, and that the different fractions reflect the relative

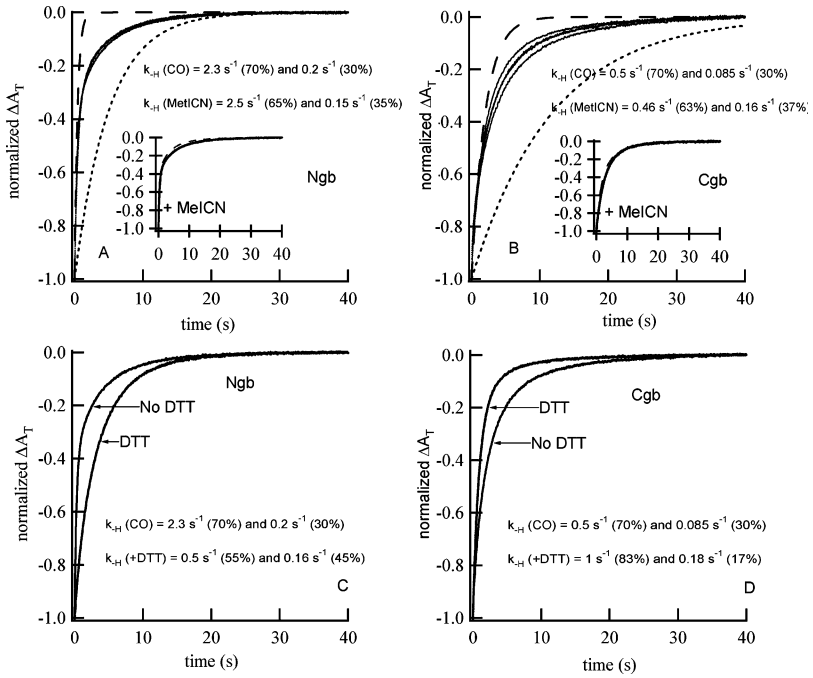

FIGURE 6: CO binding to Ngb and Cgb. Time courses for CO binding to Ngb (A) and Cgb (B) following rapid mixing at different CO concentrations (100−500 μM, right to left). In each case, the data require a double-exponential decay for proper fitting. At each concentration, a fast phase (70%) and a slow phase (30%) are observed. To demonstrate this dramatic degree of biphasic binding, the dashed and dotted lines simulate what the time courses would look like if they were described only by the fast or slow rate constant, respectively. The insets are the overlaid time courses for binding of MeICN (2 mM) and CO (500 μM), demonstrating that binding is independent of the nature of the ligand used in the experiment. Time courses of CO binding to Ngb (C) and Cgb (D) following rapid mixing at 500 μM CO with (dashed line) or without (solid line) 24 h incubation with 10 mM DTT. The time course for Ngb becomes slower, while that for Cgb is faster.

populations of oxidized and reduced protein. Hamdane et al. (*9*) reported that treatment of Ngb with DTT decreases k_{-H} (as measured by flash photolysis) to 0.6 s^{-1}. They also reported a "similar effect" in Cgb but with a smaller magnitude. An investigation of this possibility for both proteins using rapid mixing is shown in Figure 6C,D.

After a treatment of 24 h at 4 °C with 10 mM DTT (as described by Hamdane et al. (*9*)), the protein solutions were reacted with 1 mM CO. The resulting time course for Ngb is indeed slower but still exhibits two different phases of binding with nearly equal amplitudes. Surprisingly, the time course for DTT-reduced Cgb is faster and more monophasic than the untreated sample. Therefore, these results for Ngb are consistent with a disulfide bond affecting binding kinetics as described by Hamdane et al. (*9*), but this is not the cause of biphasic time courses observed for each protein. Furthermore, the direction of the subtle shift in k_{-H} for Cgb resulting from DTT shown here is opposite to that reported by Hamdane et al. (*9*).

Reactions with Other Ligands. All of the reactions measured so far have been CO binding to the ferrous form of each protein. To be sure that this behavior is not specific to this ligand, we used methyl isocyanide (MeICN) as ferrous ligand that, like CO, binds in the presence of sodium dithionite (*25*). These reactions were conducted with Ngb and Cgb because their time courses should be completely limited by k_{-H} and, thus, independent of ligand concentration and the k'_L value specific to each ligand. As shown in the inset of Figure 6A,B, no significant differences in ligand binding were observed for MeICN binding to Ngb and Cgb compared to CO. In both cases, two phases were observed with only minimal differences in the fractions of each phase compared to those for CO binding. Therefore, these experiments support assignment of the k_{obs} following rapid mixing as k_{-H}. This observation is in agreement with recent measurements of O_2 and NO binding in Ngb (*26*).

An Independent Evaluation of K_H Correlates with Values Measured by Rapid Mixing. The preceding studies were designed to provide a test of the reaction mechanism proposed in Scheme 1 by investigating time courses for ligand binding to hxHbs. The three rate constants extracted from this analysis are k_H, k_{-H}, and the bimolecular rate constant for the exogenous ligand (k'_L), in this case CO. An important affinity constant K_H can also be measured; it can be calculated as k_H/k_{-H} or extracted from eq 2 as the fraction of the reaction that binds very slowly in a rapid mixing experiment. Our results so far suggest that the slower rates of binding observed by rapid mixing are the best predictors of k_{-H} (and thus K_H). Here, we demonstrate the quantification of an independent measurement of K_H for comparison to the values we have measured kinetically.

Ferrous bis-histidyl heme has a characteristic absorption spectrum exemplified by cytochrome b_5. Plant hxHbs were the first hemoglobins to be identified with a similar spectrum (*19*, *22*). The most notable feature of this spectrum is two visible bands near 555 and 529 nm (the α and β bands, respectively) in the reduced "deoxy" absorption spectrum of the protein (Figure 7A). This is in contrast to the broad, single band near 558 nm found in most pentacoordinate Hbs (*27*). The goal of the experiment in Figure 7 is to draw a quantitative relationship between the visible absorption spectrum and K_H. To calibrate the relationship between K_H and the visible absorption spectrum, a titration of H61A soybean leghemoglobin was carried out. Wild-type soybean leghemoglobin is pentacoordinate but has a distal His side chain that blocks high-affinity imidazole binding in the

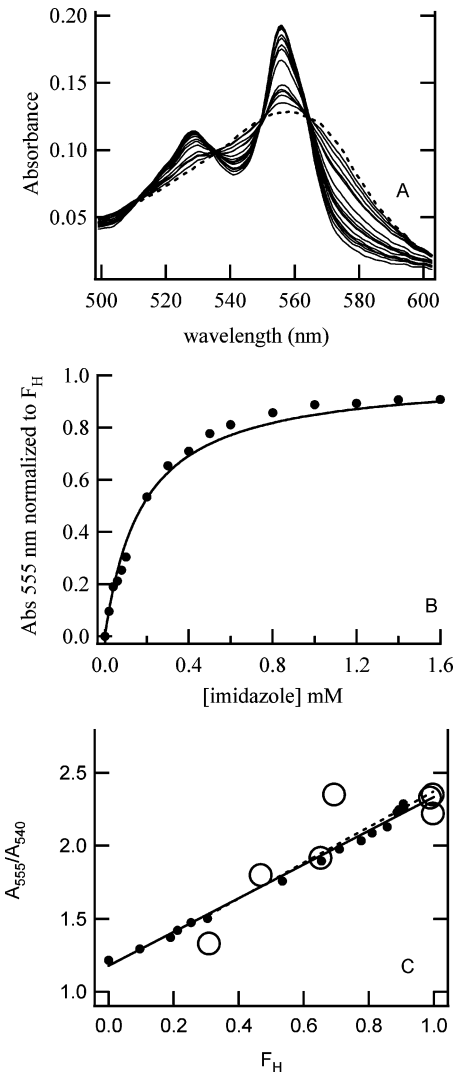

FIGURE 7: Quantification of K_H using absorbance spectroscopy. (A) Visible absorbance spectra of deoxy LbaH61A (dotted line) and LbaH61A plus imidazole (0.02−1.6 mM). (B) From a cross section of these data at 555 nm, the dissociation rate constant for imidazole was calculated to be 0.12 mM. For each imidazole concentration, the ratio of A_{555}/A_{540} is plotted versus F_H (filled circles) and fit to a line (solid line). For the hxHbs, the ratio of A_{555}/A_{540} is also plotted versus its F_H using the values listed in Table 1. A fit to these data (dashed line) is parallel to the control experiment from panel A.

ferrous form (*28*). The H61A mutant protein has a higher affinity for imidazole that facilitates titration at reasonable [imidazole]. Figure 7A shows the spectral transition from pentacoordinate to hexacoordinate heme upon imidazole addition. Figure 7B displays the normalized change in absorbance at 555 nm (reflecting F_H) along with a fitted curve depicting a K_D for imidazole of 0.12 mM. The equation used to fit this curve is provided in Materials and Methods.

A convenient feature of the absorption spectrum to correlate with F_H is one that is independent of absolute protein concentration. Therefore, the ratio of the α band (555 nm) absorbance to that at the trough between the α and β bands (540 nm) was used. The correlation of this ratio with the known F_H at each [imidazole] (calculated using the K_D of 0.12 mM) is linear for H61A leghemoglobin (Figure 7C), suggesting that A_{555}/A_{540} is a good predictor of F_H and K_H. The ratio of A_{555}/A_{540} for each hxHb is plotted versus its expected value of F_H as calculated from K_H in Table 1 (open circles in Figure 7C). While these pairs of data show more noise than those of H61A leghemoglobin, a fitted line for them lies directly on top of the control titration, suggesting that this method is a good predictor of the degree of hexacoordination in hxHbs.

DISCUSSION

In under 10 years we have seen the discovery of hxHbs in nearly all plants and animals along with cyanobacteia. The present experiments were conducted in order to clarify and consolidate ligand binding in these proteins as a class and to provide the simplest method for evaluating the rate and equilibrium constants for hexacoordination. We have demonstrated that time courses for ligand binding to this diverse collection of proteins following rapid mixing can be explained by one of three kinetic scenarios (at the top of Results). Furthermore, we have explained the complex time courses for ligand binding to the plant hxHbs as resulting from lower values of K_H and relatively rapid values of k'_{CO}. These results also demonstrate unequivocally that the hxHbs are distinct from the vertebrate hxHbs and cyanoglobin in that the latter have much higher values of K_H, exhibiting very little pentacoordinte Hb at equilibrium.

Characterization of hxHbs. The visible ferrous absorption spectrum is a very useful means for measuring F_H (and thus K_H at intermediate values). If the ratio of A_{555}/A_{540} for the dithionite-reduced hxHb is ≤ 2, the protein contains an appreciable fraction of pentacoordinate heme. If A_{555}/A_{540} is >2, the hxHb will behave more like Ngb, Cgb, and *Syn*Hb, with little F_P. This observation can serve as a convenient tool for an initial characterization of K_H in any hxHb.

Flash photolysis is the only method for measuring the bimolecular rate constant (k'_L) for ligand binding to the pentacoordinate form of the Hb (Hb_P). If there is an appreciable F_P, and k'_L is very slow, the rapid mixing experiment will not provide k'_L directly; under these conditions, the concentration dependence will be equal to $k'_L[L]/(1 + K_H)$ and one cannot resolve k'_L independently. If there is appreciable F_P and k'_L is rapid, the bimolecular reaction will likely be lost in the dead time. If there is no F_P, k'_L cannot be separated from k_H using the mixing experiment. Fortunately, no matter how complex the flash photolysis time courses appear (for example Figure 1A), k'_L is readily measurable as the dependence of the observed rate(s) on [L] (*13*).

Once k'_L is known, rapid mixing experiments can provide rate constants for hexacoordination as long as $k'_L[L]$ can be increased to the point where k_{-H} becomes limiting. This is illustrated in Figure 8 for hypothetical hxHbs with $k'_L = 10$ μM^{-1} s^{-1}, $k_{-H} = 200$ s^{-1}, and k_H varying according to the label in the figure. For the proteins with the three lower values of k_H, it would be easy to determine k_{-H} from the asymptote. Only at $k_H = 10\,000$ s^{-1} (for this example) does the time course prevent direct observation of k_{-H}. However, at high enough [L], one could overcome very large values of k_H to assign k_{-H}. Therefore, the power of this technique is limited mainly by ligand solubility. Finally, an additional benefit of eq 2 is its use of amplitudes in the analysis of stopped-flow reactions. By comparing ΔA_{obs} and ΔA_T, it is possible to measure K_H directly for hxHbs that exhibit binding according to Scenario 2.

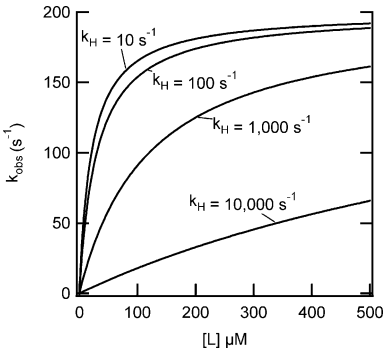

FIGURE 8: Analysis of hypothetical hxHb k_{obs} values from rapid mixing. Observed reaction rate constants are plotted as function of [L] for hypothetical hxHbs with $k_{-H} = 200\ s^{-1}$, $k'_L = 10\ s^{-1}$, and k_H as indicated in the figure for each curve. The asymptote used to assign k_{-H} is obvious in all cases accept that where $k_H = 10\,000\ s^{-1}$. Under these circumstances, binding is as described by Scenario 3 of Results. This simulation illustrates the degree to which k_H must be very large compared to k'_L[L] to interfere with the ability of rapid mixing experiments to extract rate constants for hexacoordination.

Additional Binding Phases Observed by Flash Photolysis. While the results presented here clarify binding following rapid mixing and demonstrate that these rate constants correlate with K_H at equilibrium, we are left with the question of the cause of the multiphasic time courses following flash photolysis in many hxHbs. One possible explanation is different protein conformations with microscopic values of k_H and k_{-H}. The crystal structures of *Syn*Hb in the presence and absence of bound ligand support this possibility (*29*). When an exogenous ligand is bound, His[46] (which coordinates the ligand binding site in the absence of exogenous ligands) moves completely out of the heme pocket and is accompanied by major rearrangements in the B and E helices and the EF loop (*30*). It is possible that the conformational change that facilitates hexacoordination following flash photolysis follows more than one pathway, causing heterogeneity in the time course for ligand rebinding.

Alternatively, solvent or another amino acid side chain could transiently coordinate the heme following ligand photolysis causing multiphasic time courses. This possibility is supported by the absorbance spectrum of the H46L and H64L mutant proteins of *Syn*Hb (*16*) and Ngb, respectively (*11*, *16*). These are the hexacoordinating His side chains in each, and the mutant proteins show coordination of some other ligand (presumably solvent) in the absence of exogenous ligands. Finally, an unusually large amount of room-temperature geminate rebinding of CO could also cause heterogeneous time courses following flash photolysis (*11*, *16*).

Plant hxHbs. Plant hxHbs have surprising variability in kinetics within and across species given their high degree of sequence conservation. The variability in k'_{CO} is much larger than that for myoglobin from different animals (*27*). This is consistent with results published earlier for the *Arabidopsis* Hbs where two hxHbs (GLB1 and GLB2) and one trHb (GLB3) are found with dissimilar expression patterns (*31*, *32*). Consideration of both expression patterns and kinetics results suggests that Hbs inside the same plant could have different functions in the specific regions where they are expressed (*31*).

Alternatively, plant hxHbs could exhibit kinetic variability in the absolute values of some rate constants but have the same function due to the specific combinations found in any particular plant. This is true for plant leghemoglobins. Soybean and lupin leghemoglobin have quite different rate constants for oxygen binding, but the specific combinations of association and dissociation rate constants in each give them the same overall affinity constants for oxygen that are necessary for their common function in root nodules (*28*, *33*).

Each of the plant hxHbs exhibits ~5−10% of the expected ΔA_T that is slow (~1 s^{-1}). This has been observed previously (*17*), and the cause is not obvious. It is notable that this rate is near that of the faster k_{-H} values for Ngb and Cgb. This suggests that the coordinating His might spend a small fraction of its time locked into a tighter bond with the heme iron that is more similar to the structures observed for Ngb and Cgb (*34*, *35*).

Human hxHbs. Ngb and Cgb are two very different hxHbs (*36*). They are expressed in different tissues and their kinetic and affinity constants for oxygen and CO are quite different. But with respect to hexacoordination, they share some common features that are distinct from the plant hxHbs. Both have comparatively slow values for k_{-H} and subsequently higher values of K_H. Both also have a much larger degree of unexplained time course heterogeneity than the plant hxHbs. One possible explanation for this in Ngb is different conformations of the bound His[64] (*37*, *38*). The structure of the murine Ngb displays two different conformations for the heme iron associated with two tautomers for the distal histidine. These conformations were found at a ratio of 70:30, exactly that reported here for the ratio of absorbance amplitudes describing the fast and slow fractions of the time courses for CO binding.

It has been shown that CO binding induces a major heme displacement accompanied by a rearrangement of the EF−F−FG region and the CD loop (*10*, *37*, *38*). It has also been shown that the disulfide bond in the CD region can affect the kinetics of hexacoordination by lowering k_{-H} for Ngb (*9*). Our results suggest that this effect is not the same for Cgb, where an increase in k_{-H} was observed in the presence of DTT. So, it seems that the E-helix and the CD region are important in controlling the ligand affinity but that the effect of rearrangement is specific to each protein.

In conclusion, the results presented here clarify our understanding of ligand binding in hxHbs in three ways. First, they demonstrate that the slower phases of CO binding following rapid mixing are the best estimate of k_{-H}, as it is these values that correlate with an independent spectroscopic measurement of K_H. Second, they present a mechanistically simple explanation for multiphasic time courses in hxHbs that have appreciable fractions of pentacoordinate heme. Finally, the direct comparison of hxHbs from plants, animals, and bacteria using these methods indicate that the plant hxHbs have much lower values of K_H than the others.

REFERENCES

1. Burmester, T., Welch, B., Reinhardt, S., and Hankeln, T. (2000) A vertebrate globin expressed in the brain, *Nature 407*, 520−523.
2. Wittenberg, J. B., Bolognesi, M., Wittenberg, B. A., and Guertin, M. (2002) Truncated hemoglobins: a new family of hemoglobins

widely distributed in bacteria, unicellular eukaryotes, and plants, *J. Biol. Chem. 277*, 871−874.
3. Appleby, C. (1992) The origin and functions of hemoglobin in plants, *Sci. Prog. 76*, 365−398.
4. Kundu, S., Trent, J. T., III, and Hargrove, M. S. (2003) Plants, humans, and hemoglobins, *Trends Plant Sci. 8*, 387−393.
5. Trent, J. T., III, and Hargrove, M. S. (2002) A ubiquitously expressed human hexacoordinate hemoglobin, *J. Biol. Chem. 277*, 19538−19545.
6. Trent, J. T., III, Watts, R. A., and Hargrove, M. S. (2001) Human neuroglobin, a hexacoordinate hemoglobin that reversibly binds oxygen, *J. Biol. Chem. 276*, 30106−30110.
7. Hargrove, M., Brucker, E., Stec, B., Sarath, G., Arredondo-Peter, R., Klucas, R., Olson, J., and Phillips, G. (2000) Crystal structure of a nonsymbiotic plant hemoglobin, *Struct. Fold Des. 8*, 1005−1014.
8. Hamdane, D., Kiger, L., Dewilde, S., Uzan, J., Burmester, T., Hankeln, T., Moens, L., and Marden, M. C. (2005) Hyperthermal stability of neuroglobin and cytoglobin, *FEBS J. 272*, 2076−2084.
9. Hamdane, D., Kiger, L., Dewilde, S., Green, B. N., Pesce, A., Uzan, J., Burmester, T., Hankeln, T., Bolognesi, M., Moens, L., and Marden, M. C. (2003) The redox state of the cell regulates the ligand binding affinity of human neuroglobin and cytoglobin, *J. Biol. Chem. 278*, 51713−51721.
10. Kriegl, J. M., Bhattacharyya, A. J., Nienhaus, K., Deng, P., Minkow, O., and Nienhaus, G. U. (2002) Ligand binding and protein dynamics in neuroglobin, *Proc. Natl. Acad. Sci. U.S.A. 99*, 7992−7997.
11. Nienhaus, K., Kriegl, J. M., and Nienhaus, G. U. (2004) Structural dynamics in the active site of murine neuroglobin and its effects on ligand binding, *J. Biol. Chem. 279*, 22944−22952.
12. Dewilde, S., Kiger, L., Burmester, T., Hankeln, T., Baudin-Creuza, V., Aerts, T., Marden, M. C., Caubergs, R., and Moens, L. (2001) Biochemical characterization and ligand binding properties of neuroglobin, a novel member of the globin family, *J. Biol. Chem. 276*, 38949−38955.
13. Hargrove, M. S. (2000) A flash photolysis method to characterize hexacoordinate hemoglobin kinetics, *Biophys. J. 79*, 2733−2738.
14. Kundu, S., Premer, S., Hoy, J., Trent, J. T., III, and Hargrove, M. (2003) Direct measurement of equilibrium constants for high-affinity hemoglobins, *Biophys J. 84*, 3931−3940.
15. Olson, J. S. (1981) Stopped-flow, rapid mixing measurements of ligand binding to hemoglobin and red cells, *Methods Enzymol. 76*, 631−651.
16. Hvitved, A. N., Trent, J. T., III, Premer, S. A., and Hargrove, M. S. (2001) Ligand binding and hexacoordination in *Synechocystis* hemoglobin, *J. Biol. Chem. 276*, 34714−34721.
17. Trent, J. T., III, Hvitved, A. N., and Hargrove, M. S. (2001) A model for ligand binding to hexacoordinate hemoglobins, *Biochemistry 40*, 6155−6163.
18. Weber, R. E., and Fago, A. (2004) Functional adaptation and its molecular basis in vertebrate hemoglobins, neuroglobins and cytoglobins, *Respir. Physiol. Neurobiol. 144*, 141−159.
19. Arrendondo-Peter, R., Hargrove, M. S., Sarath, G., Moran, J. F., Lohrman, J., Olson, J. S., and Klucas, R. V. (1997) Rice hemoglobins. Gene cloning, analysis, and O_2-binding kinetics of a recombinant protein synthesized in *Escherichia coli*, *Plant Physiol. 115*, 1259−1266.
20. Ross, E. J. H. (2002) Plant nonsymbiotic hemoglobins: Hexacoordinated hemoglobins involved in hormonally-regulated cell differentiation, Ph.D. Dissertation.
21. Hargrove, M. S. (2000) A flash photolysis method to characterize hexacoordinate hemoglobin kinetics, *Biophys. J. 79*, 2733−2738.
22. Duff, S. M. G., Wittenberg, J. B., and Hill, R. D. (1997) Expression, purification, and properties of recombinant barley (*Hordeum* sp.) hemoglobin, *J. Biol. Chem. 272*, 16746−16752.
23. Goodman, M. D., and Hargrove, M. S. (2001) Quaternary structure of rice nonsymbiotic hemoglobin, *J. Biol. Chem. 276*, 6834−6839.
24. Hamdane, D., Kiger, L., Dewilde, S., Green, B. N., Pesce, A., Uzan, J., Burmester, T., Hankeln, T., Bolognesi, M., Moens, L., and Marden, M. C. (2004) Coupling of the heme and an internal disulfide bond in human neuroglobin, *Micron 35*, 59−62.
25. Olson, J. S., Mathews, A. J., Rohlfs, R. J., Springer, B. A., Egeberg, K. D., Sligar, S. G., Tame, J., Renaud, J. P., and Nagai, K. (1988) The role of the distal histidine in myoglobin and haemoglobin, *Nature 336*, 265−266.
26. Brunori, M., Giuffre, A., Nienhaus, K., Nienhaus, G. U., Scandurra, F. M., and Vallone, B. (2005) Neuroglobin, nitric oxide, and oxygen: Functional pathways and conformational changes, *Proc. Natl. Acad. Sci. U.S.A. 102*, 8483−8488.
27. Antonini, E., and Brunori, M. (1971) *Hemoglobin and Myoglobin in Their Reactions with Ligands*, Vol. 21, North-Holland Publishing Company, Amsterdam.
28. Kundu, S., and Hargrove, M. S. (2003) Distal heme pocket regulation of ligand binding and stability in soybean leghemoglobin, *Proteins 50*, 239−248.
29. Trent, J. T., III, Kundu, S., Hoy, J. A., and Hargrove, M. S. (2004) Crystallographic analysis of *Synechocystis* cyanoglobin reveals the structural changes accompanying ligand binding in a hexacoordinate hemoglobin, *J. Mol. Biol. 341*, 1097−1108.
30. Vu, B., Nothnagel, H., Vuletich, D. A., Falzone, C. J., and Lecomte, J. T. J. (2004) Cyanide binding to hexacoordinate cyanobacterial hemoglobins: hydrogen-bonding network and heme pocket rearrangement in ferric H117A Synechocystis hemoglobin., *Biochemistry 43*, 12622−12633.
31. Hunt, P. W., Watts, R. A., Trevaskis, B., Llewellyn, D. J., Burnell, J., Dennis, E. S., and Peacock, W. J. (2001) Expression and evolution of functionally distinct haemoglobin genes in plants, *Plant Mol. Biol. 47*, 677−692.
32. Watts, R., Hunt, P., Hvitved, A., Hargrove, M., Peacock, W., and Dennis, E. (2001) A hemoglobin from plants homologous to truncated hemoglobins of microorganisms, *Proc. Natl. Acad. Sci. U.S.A. 98*, 10119−10124.
33. Kundu, S., Snyder, B., Das, K., Chowdhury, P., Park, J., Petrich, J. W., and Hargrove, M. S. (2002) The leghemoglobin proximal heme pocket directs oxygen dissociation and stabilizes bound heme, *Proteins 46*, 268−277.
34. de Sanctis, D., Dewilde, S., Pesce, A., Moens, L., Ascenzi, P., Hankeln, T., Burmester, T., and Bolognesi, M. (2004) Crystal structure of cytoglobin: the fourth globin type discovered in man displays heme hexa-coordination, *J. Mol. Biol. 336*, 917−927.
35. Pesce, A., Dewilde, S., Nardini, M., Moens, L., Ascenzi, P., Hankeln, T., Burmester, T., and Bolognesi, M. (2003) Human brain neuroglobin structure reveals a distinct mode of controlling oxygen affinity, *Structure 9*, 1087−1095.
36. Hankeln, T., Ebner, B., Fuchs, C., Gerlach, F., Haberkamp, M., Laufs, T. L., Roesner, A., Schmidt, M., Weich, B., and Wystub, S. (2005) Neuroglobin and cytoglobin in search of their role in the vertebrate globin family, *J. Inorg. Biochem. 99*, 110−119.
37. Vallone, B., Nienhaus, K., Brunori, M., and Nienhaus, G. U. (2004) The structure of murine neuroglobin: Novel pathways for ligand migration and binding, *Proteins 56*, 85−92.
38. Vallone, B., Nienhaus, K., Matthes, A., Brunori, M., and Nienhaus, G. U. (2004) The structure of carbonmonoxy neuroglobin reveals a heme-sliding mechanism for control of ligand affinity, *Proc. Natl. Acad. Sci. U.S.A. 101*, 17351−17356.

BI051902L